Structural Alterations in Deep Brain Structures in Type 1 Diabetes

Pavel Filip,[1,2,3] Antonietta Canna,[1,4] Amir Moheet,[5] Petr Bednarik,[1,6] Heidi Grohn,[1,7] Xiufeng Li,[1] Anjali F. Kumar,[5] Evan Olawsky,[8] Lynn E. Eberly,[8] Elizabeth R. Seaquist,[5] and Silvia Mangia[1]

Diabetes 2020;69:2458–2466 | https://doi.org/10.2337/db19-1100

Even though well known in type 2 diabetes, the existence of brain changes in type 1 diabetes (T1D) and both their neuroanatomical and clinical features are less well characterized. To fill the void in the current understanding of this disease, we sought to determine the possible neural correlate in long-duration T1D at several levels, including macrostructural, microstructural cerebral damage, and blood flow alterations. In this cross-sectional study, we compared a cohort of 61 patients with T1D with an average disease duration of 21 years with 54 well-matched control subjects without diabetes in a multimodal MRI protocol providing macrostructural metrics (cortical thickness and structural volumes), microstructural measures (T1-weighted/T2-weighted [T1w/T2w] ratio as a marker of myelin content, inflammation, and edema), and cerebral blood flow. Patients with T1D had higher T1w/T2w ratios in the right parahippocampal gyrus, the executive part of both putamina, both thalami, and the cerebellum. These alterations were reflected in lower putaminal and thalamic volume bilaterally. No cerebral blood flow differences between groups were found in any of these structures, suggesting nonvascular etiologies of these changes. Our findings implicate a marked nonvascular disruption in T1D of several essential neural nodes engaged in both cognitive and motor processing.

Type 1 diabetes (T1D) is a chronic autoimmune disease stemming from the interactions of predisposing polygenic traits with ill-defined environmental factors. The combination of inherent hyperglycemic and treatment-induced hypoglycemic states, both transient and long term, leads to clinically relevant damage of multiple organs, including blood vessels, heart, kidneys, eyes, and even the central nervous system (CNS). Although a source of major concern in type 2 diabetes in an aging population, the risk of CNS damage in T1D is often marginalized. Nonetheless, multiple studies indicate subtle, but definitive differences in several domains of cognition, mainly slowing of mental speed and decreased mental flexibility (1). While psychosocial factors related to behavior (2) and school attendance (3) have been proposed as potential contributors, diabetes-related organic factors are usually stated in light of imaging and electrophysiological studies, giving rise to the concept of "diabetic encephalopathy," even in T1D (4).

The ways in which diabetes and its treatments could affect the brain are numerous. The human brain vitally depends on continuous glucose availability and rapidly malfunctions in cases of significant deviations from the normal range, but the long-term consequences of these events are difficult to define. Protracted severe hypoglycemia is rather rare, but the risk of permanent cognitive and neurological deficits, even associated with localized neuroimaging abnormalities in temporal lobes and deep gray matter (GM) (5), is not negligible. Conversely, there are several toxic effects of hyperglycemia, including nonenzymatic protein glycosylation (6), oxidative stress (7),

[1]Center for Magnetic Resonance Research, University of Minnesota, Minneapolis, MN
[2]Department of Neurology, Charles University, First Faculty of Medicine and General University Hospital, Prague, Czech Republic
[3]First Department of Neurology, Faculty of Medicine, Masaryk University and University Hospital of St. Anne, Brno, Czech Republic
[4]Department of Medicine, Surgery and Dentistry, Scuola Medica Salernitana, University of Salerno, Salerno, Italy
[5]Department of Medicine, University of Minnesota, Minneapolis, MN
[6]High Field MR Centre, Department of Biomedical Imaging and Image-guided Therapy, Medical University of Vienna, Vienna, Austria
[7]Diagnostic Imaging Center, Kuopio University Hospital, Kuopio, Finland
[8]Division of Biostatistics, School of Public Health, University of Minnesota, Minneapolis, MN

Corresponding author: Silvia Mangia, mangia@umn.edu

Received 3 November 2019 and accepted 19 August 2020

This article contains supplementary material online at https://doi.org/10.2337/figshare.12840641.

and disturbed Ca^{2+} homeostasis (8), leading to blood flow impairments and angiopathy. The consequences of hyperglycemia at the neural level include not only alterations of neurotrophic modulators but also deep changes in gene transcription in the hypothalamus and hippocampus (9). Furthermore, T1D, as well as type 2 diabetes, seems to exert a negative effect on GAD levels (10), the principal enzyme responsible for γ-aminobutyric acid (GABA) synthesis. Because the majority of striatal neurons and a nonnegligible proportion of neocortical neuronal populations are GABA-ergic interneurons with significant modulatory effects, diabetes may affect a vast spectrum of neural circuits and functions, ranging from cognition to sensorimotor processing (11). Finally, the autoimmune nature of T1D must be taken into account since the lymphocytes targeting proteins expressed by pancreatic β-cells (antibodies to islet cells, insulin, GAD, or protein tyrosine phosphatase [12], to name the major examples) show a conspicuous lack of tissue and disease fidelity; celiac disease, thyroid gland autoimmunity, and Addison disease are not uncommon in patients with T1D (13). Specifically, anti-GAD antibodies have been identified as a causal agent in multiple CNS affections, with detrimental effects reported mainly for Purkinje cells in the cerebellum (14).

The current body of brain imaging research in T1D is largely limited to descriptive and volumetric studies. The reports of both cerebral white matter (WM) lesions representing focal ischemia and gliosis (4,15–17) and the absence of any WM alterations (18) are usually limited by smaller sample sizes. Volumetric studies also display certain levels of heterogeneity, implicating GM volume reductions in frontal and temporal lobes (19,20), whole cortex with maximum in the frontal lobes (21), and occipital and frontal cortices (22). Thalamic atrophy in T1D has also been reported and suggested to be associated with cognitive deficits (23). Moreover, while hippocampal volume increase has been reported in children with T1D after higher exposure to severe hypoglycemia (24), a significant number of cases of mesial temporal sclerosis (i.e., hippocampal region atrophy usually associated with temporal lobe epilepsy) (25) without previous history of severe hypoglycemia have been identified in patients with T1D. Hypoglycemic coma also has been linked to lesions in basal ganglia, the hippocampus, and several cortical regions (24). Furthermore, relatively higher total cerebral blood flow (CBF) has been reported in T1D (26).

Thus, the aim of our cross-sectional study was to investigate the effects of T1D in the brain at both the macrostructural and the microstructural level. While macrostructural changes (volumetric and cortical thickness changes) were analyzed using T1-weighted (T1w) and T2-weighted (T2w) MRI scans, microstructural analysis was based on the T1w/T2w ratio, a compound derivative reflecting cortical GM myelin content (27), an increase in water as a result of inflammation or edema, and alterations in iron content (28). The very nonspecificity of this measure to a single pathological process makes it ideal for probing analyses to detect a wide spectrum of hypothesized changes. Finally, CBF, a parameter highly relevant in the context of possible T1D-associated angiopathy, was used to provide further information on the potential etiology of CNS changes and their relation to blood supply changes. Building on the previous body of research, we hypothesized that macrostructural changes, mainly in the frontal cortex, hippocampus, GABA-ergic striatum, and cerebellum as a region prone to autoimmune damage in T1D, will be seen concurrently with an altered T1w/T2w ratio, reflecting the underlying and possibly preceding microstructural damage, and by smaller CBF, as a result of the generalized T1D-associated angiopathy as one of the eventual causal factors for these alterations. While microstructural and/or macrostructural changes associated with decreased CBF would indicate vascular etiology of the detected alterations, the absence of significant CBF changes in combination with microstructural and/or macrostructural differences could point to other causes with reasonable uncertainty related to the sensitivity of CBF to detect microangiopathy-associated blood flow alterations.

RESEARCH DESIGN AND METHODS

Subjects

Data sets were retrospectively drawn from experiments that were conducted over a time frame of 5 years from 2015 to 2020 within a completed project that aimed to describe the brain responses to hypoglycemia during hyperinsulinemic clamps. Only studies with complete and consistently acquired T1w and T2w structural MRI were considered in this analysis.

Overall, 63 patients with T1D were included. The inclusion criteria were presence of T1D (defined on clinical grounds) and glycated hemoglobin (HbA_{1c}) level $<9\%$ in the 3 months before study participation. Demographics (sex, age) and basic information about T1D (including disease duration) were based on patient report. Blood samples for HbA_{1c} were collected on the day of the study. Additionally, 56 control subjects without diabetes of corresponding age and sex to match the T1D group were included. Exclusion criteria were proliferative retinopathy, comorbid neurological or severe psychiatric diseases, MRI contraindications, and significant vascular or space-occupying lesions on MRI scans. There was a partial overlap with the previously published study cohort (21) in that 24 patients with T1D and 31 control subjects without diabetes were shared in the present and previously published reports. The remaining subjects from the previous report could not be included in the present analysis because of differences in T2w sequence, which was updated during the course of the whole project, leading to substantial changes in the main parameter of interest of this study: the T1w/T2w ratio (see Supplementary Fig. 1 for further information).

This study was performed in accordance with the recommendations of the Code of Federal Regulations. The protocol was approved by the institutional review

board human subjects committee of the University of Minnesota. Each subject provided written informed consent in accordance with the Declaration of Helsinki.

Imaging Protocol

The MRI acquisition was performed using the 3T Siemens MAGNETOM Prisma system (Siemens, Erlangen, Germany). T1w images were acquired using the magnetization-prepared rapid gradient-echo (MPRAGE) sequence, with voxel size = $1 \times 1 \times 1$ mm^3, repetition time = 2,150 ms, echo time (TE) = 2.47 ms, inversion time = 1,000 ms, generalized autocalibrating partial parallel acquisition = 2, and flip angle = 8°. The acquisition of T2w images was based on the SPACE sequence, with voxel size = $1 \times 1 \times 1$ mm^3, TE = 147 ms, and generalized autocalibrating partial parallel acquisition = 2. No prescan normalization algorithm as implemented by the manufacturer was used in T1w or T2w scans. Finally, the pseudocontinuous arterial spin labeling sequence was acquired with a repetition time = 5,000 ms, TE = 14 ms, field of view = 210×210 mm^2, voxel size = $3 \times 3 \times 3$ mm^3, number of slices = 36 with 20% gap, labeling plane thickness = 10 mm, labeling plane offset = 90 mm, labeling duration = 1,600 ms, labeling postlabeling delay = 1,600 ms, and number of pairs of label/control images = 80 (in 10 subjects, the number of label/control pairs was 79). The metabolic condition during the MRI acquisition was controlled using a hyperinsulinemic clamp to maintain blood glucose level of ~95 mg/dL (for details of the procedure, see Mangia et al. [29]).

Image Processing

The structural analysis was based on the state-of-the-art Human Connectome Project (HCP) minimal preprocessing pipeline (30), which consisted of the PreFreeSurfer (including gradient distortion correction), FreeSurfer (FreeSurfer 5.3-HCP; https://surfer.nmr.mgh.harvard.edu), and PostFreeSurfer steps. The accuracy of the segmentation and parcellation in each subject was visually inspected (P.F.). Two patients with T1D and two control subjects without diabetes were excluded from further analyses because of low quality of imaging data and/or irrecoverable processing failure, leaving 61 processable scans from patients with T1D and 54 control subjects (see Supplementary Fig. 2 for the enrollment). We implemented the combined volumetric and surface–based registration (31,32), an advanced nonlinear registration algorithm surpassing the procedures implemented in the HCP pipeline. Cortical thickness surface maps as provided by the HCP pipeline and volumes of relevant regions of interest (ROIs) were used for the analysis of cortical thickness and volume differences, respectively. The following regions of interest were included as implicated in the previous body of research in T1D: striatum (distinguishing among its main parts: putamen, pallidum, and caudate), cerebellar GM, cortical GM (distinguishing among the frontal, parietal, temporal, and occipital lobes), hippocampus, and thalamus. Estimated intracranial volumes were used to adjust ROI volumes to the head size.

Voxel-based morphometry (VBM) analysis was also performed with SPM12 (Wellcome Trust Centre for Neuroimaging, London, U.K.; https://www.fil.ion.ucl.ac.uk/spm) in MATLAB R2016 (MathWorks, Natick, MA). T1w images were segmented into the three different tissue classes of GM, WM, and cerebrospinal fluid. The diffeomorphic registration algorithm DARTEL (33) was used to normalize the GM probabilistic maps to the Montreal Neurological Institute (MNI) space with 2-mm isotropic resolution. The resulting images were then modulated by multiplying the GM voxels by the Jacobians derived from the corresponding spatial normalization parameters. A 4-mm full-width half-maximum Gaussian kernel was used to avoid overestimating the eventual effects, considering the size of the analyzed cohort (34). Areas of significant difference between the T1D and control groups as detected by VBM were considered secondary ROIs for the analysis of volume differences using the FreeSurfer output to verify the results through a second method and eventually increase the robustness of reported outcomes.

T1w/T2w ratio analysis was based on the volume images and T1w/T2w ratio surface maps (also known as myelin maps) of the whole cortex generated by the HCP preprocessing pipeline. An HCP pipeline–derived mask of WM and subcortical structures was used to remove the cortical voxels from the T1w/T2w ratio volume images. The created "decorticated" images were then downsampled to 2-mm isotropic resolution and warped to the MNI space using the combined volumetric and surface–generated matrix. Afterward, these MNI-registered T1w/T2w ratio scans were combined with the myelin maps to create Connectivity Informatics Technology Initiative (CIFTI) files.

Harvard-Oxford subcortical structural atlas, Oxford-Imanova striatal connectivity atlas, and cerebellar atlas as implemented in FSL (Functional Magnetic Resonance Imaging of the Brain Software Library) were used for the classification and localization of significant clusters in the MNI space. For the CBF processing pipeline, see the Supplementary Material.

ROIs

ROIs were selected on the basis of the scientific background described above, and their masks were obtained after the minimal preprocessing HCP pipeline. The ROIs included the bilateral caudate, putamen, pallidum, thalamus, hippocampus, cerebellum, and four lobes of the neocortex, namely the frontal cortex, parietal cortex, temporal cortex, and occipital cortex. The sum of the neocortex was also separately considered and referred to as the whole cortex.

FreeSurfer volumetry and CBF outcomes were evaluated in these ROIs to provide supportive evidence to the voxel-based analyses. ROI volumes divided by the estimated intracranial volume (as provided by FreeSurfer) were considered for this analysis. In CBF analysis, because

of the bigger dimension of the thalamus and the heterogeneity of this region compared with the other subcortical structures, the mask in the bilateral thalamus was eroded by 1 voxel. The ROI masks were each coregistered to the CBF maps in a two-step procedure: *1*) the mean control volume of the pseudocontinuous arterial spin labeling series was linearly coregistered to the T1w image using the FLIRT (Functional Magnetic Resonance Imaging of the Brain Linear Image Registration Tool) command with trilinear interpolation, and then *2*) the inverse of the transformation matrix was applied to each of the ROI masks. For each subject and ROI, within-ROI mean and SD values were computed before and after excluding the outliers of the CBF distribution in the ROI (i.e., before and after excluding the values outside the range), as follows: 25th percentile − 1.5 * interquartile; 75th percentile + 1.5 * interquartile.

Statistical Analyses

Equivalence analysis (two one-sided tests) was used to verify the equivalence of sex and age distributions between the patients with T1D and control subjects without diabetes to avoid type II errors, with $P < 0.05$ considered statistically significant. Group differences of 33% and 10 years for sex and age, respectively, were considered clinically relevant. Quantitative clinical data were summarized using descriptive statistics.

General linear models (GLMs) were used to compare outcomes between groups, with sex and age as covariates of noninterest. For the group comparison of VBM maps, cortical thickness maps, and T1w/T2w ratio CIFTI images (consisting of surface maps and subcortical structures), we used permutation-based nonparametric statistical methods as implemented in the Permutation Analysis of Linear Models package (35), running 5,000 permutations with threshold-free cluster enhancement and adjustment using the average area per vertex. In addition to sex and age, the GLM model in the VBM included also the intracranial volume as a nuisance variable. Furthermore, secondary analyses in the T1D group correlating disease duration and long-term blood glucose control (HbA_{1c} level) with VBM, cortical thickness, and T1w/T2w ratio were performed with age and sex as nuisance variables.

In the GLM analysis of VBM, $P < 0.05$ familywise error (FWE) with threshold-free cluster enhancement of voxelwise correction was used. In the GLM analysis of the combined surface and volume CIFTI files, $P < 0.05$ FWE correction with subsequent Bonferroni correction (because of the two and three individual components in the cortical thickness and T1w/T2w ratio CIFTI files, respectively) was implemented.

For the ROI analyses of CBF and FreeSurfer volumetry outcomes, one between-subject (two levels for control subjects without diabetes and T1D) ANOVA was performed on the ROI-specific mean outcomes after regressing out age, sex, and BMI. Similar to the analyses for T1w/T2w ratio, cortical thickness, and VBM, secondary correlation analyses were also computed for the FreeSurfer volumetry outcomes and CBF values in the ROIs with disease duration and HbA_{1c} level in the patients with T1D, again after regressing out the effect of age and sex.

We implemented Holm correction with $P < 0.05$ across the considered ROIs, 10 comparisons for the volumetry outcomes (bilateral caudate, putamen, pallidum, hippocampus, cerebellum, thalamus, frontal lobe, parietal lobe, occipital lobe, temporal lobe), and 9 comparisons for the CBF outcomes (where we did not include the cerebellum because the CBF coverage of this region was not consistent among subjects). The whole cortex region was not subjected to multiple comparison corrections. Results are presented before and after type I error adjustment using Holm correction.

Data and Resource Availability

The data sets generated during the current study are not publicly available because of the sensitive nature of human data acquired in patients, but they are available from the corresponding author upon reasonable request.

RESULTS

The two one-sided tests confirmed the equivalence of both sex and age distributions in the two study groups. Demographic and basic clinical information in patients with T1D is provided in Table 1.

In the structural analysis, the VBM approach revealed lower GM volume in patients with T1D in both putamina (major components of the striatum) (Fig. 1*A* and Table 2). According to the colocation with the connectivity atlases, these changes affected predominantly executive parts of striatum (Table 2). The reverse contrast (patients with T1D > control subjects without diabetes) did not reveal any differences significant at the predetermined level.

The analysis of myelin maps revealed an increased T1w/T2w ratio in patients with T1D in the area of the right fusiform and parahippocampal gyrus (Fig. 1*C*) and alterations in bilateral striatum (mainly putamen and caudate head) and thalamus (Fig. 1*B* and Table 2). According to the collocation with the connectivity atlases, these differences affected predominantly executive and limbic parts of striatum and thalamic areas communicating predominantly with posterior parietal and prefrontal cortices. Furthermore, a similarly higher T1w/T2w ratio was observed in both the anterior (lobules I-IV) and posterior cerebellum (lobules VII, VIII) bilaterally (Table 2 and Fig. 1*B*). The reverse contrast (i.e., control subjects without diabetes > patients with T1D) failed to reveal any significant clusters.

The comparison of cortical thickness failed to detect any differences between the control subjects without diabetes and patients with T1D. Smaller volumes of putamen ($P = 0.025$, corrected) and thalamus ($P < 0.0001$, corrected) were observed in the patients with T1D compared with the control subjects (Table 3).

Table 1—Demographics and clinical characteristics of study subjects

	Control subjects without diabetes	Patients with T1D
n	54	61
Sex (female/male), *n*	26/28	34/27
Age (years)	35 ± 13 (18–63)	36 ± 13 (18–67)
HbA_{1c}, %	5.2 ± 0.3 (4.6–5.9)	7.4 ± 1.2 (5.6–13.6)
BMI (kg/m^2)	25.6 ± 4.5 (17.5–40.9)	26.3 ± 4.2 (18.9–38.8)
Disease duration (years)	—	21 ± 11 (1–45)
Age at diagnosis (years)	—	15 ± 10 (2–49)
History		
Hypertension	0	7 (12)
Dyslipidemia	0	7 (14)
Hypothyroidism	0	11 (18)
Asthma	1 (2)	3 (6)
Celiac disease	0	3 (6)
Depression	1 (2)	9 (16)

Data are mean ± SD (range) or *n* (%) unless otherwise indicated.

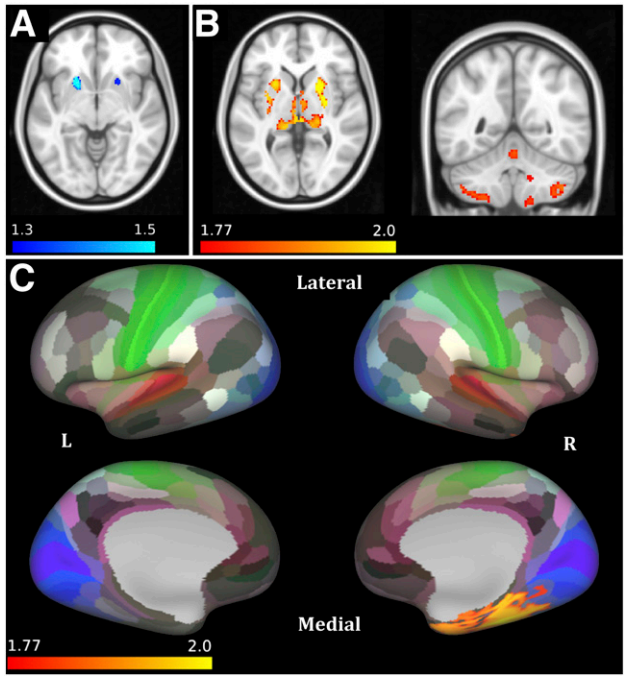

Figure 1—Results of voxel-based morphometry (VBM) and the T1w/T2w ratio between-group comparison, permutation-based analysis with threshold-free cluster enhancement. Clusters are significant at $P < 0.05$ familywise error (FWE) and FWE + Bonferroni voxel (gray ordinate)-wise corrected for VBM and T1w/T2w ratio, respectively; log-*P* scale, with the cluster threshold of 50 contiguous voxels in voxel-based analyses. *A*: VBM: control subjects without diabetes > patients with T1D; blue color pattern shows lower gray matter in both putamina in patients with T1D. *B*: T1w/T2w ratio: patients with T1D > control subjects without diabetes, with higher T1w/T2w ratio in both putamina, thalami, and the cerebellum. *C*: T1w/T2w ratio: patients with T1D patients > control subjects without diabetes, showing inflated average surface HCP template with overlaid HCP multimodal parcellation. Higher T1w/T2w ratio in the right fusiform and parahippocampal gyrus. Conventions for the laterality were used where the right side in the panel corresponds to the right side in the scanned area. See Table 2 for detailed statistical results and anatomical localization of clusters. L, left; R, right.

No differences in CBF between the two groups were found in the above-stated ROIs (Table 4). The supplementary CBF analysis using less restrictive scrubbing criteria (see RESEARCH DESIGN AND METHODS) performed for 52 control subjects without diabetes and 58 patients with T1D that survived to the exclusion criteria defined above confirmed the absence of statistically significant differences between subjects with and without diabetes. Similarly, no statistically significant CBF differences were found when considering data without removing the outliers. The secondary analyses in the T1D group correlating disease duration and blood glucose control (HbA_{1c} level) with ROI volumes, cortical thickness, CBF, and T1w/T2w ratio provided no significant results.

DISCUSSION

Our study, the first to investigate brain alterations in T1D on macrostructural, microstructural, and CBF levels simultaneously, reveals significant differences between participants with T1D and control subjects without diabetes in the striatum, thalamus, and mesial temporal cortex—core structures essential for multiple aspects of cognition and executive and motor functions. Importantly, while the adopted measure of microstructural changes (T1w/T2w ratio) found clear changes in multiple areas, alterations in macrostructural integrity were far less prominent and present only in the areas revealed in the T1w/T2w ratio assessment. Although surprising considering the dominant affection in deep brain regions and the pathophysiological characteristics of T1D with increased vascular risks, this encroachment of T1D-associated pathological processes into the CNS was not reflected in alterations of CBF, suggesting that another etiology may contribute to microstructural disruptions noted in diabetes.

Of particular interest is whether relevant functional impairments could be associated with these pathological alterations in striatal, thalamic, and neocortical neuronal circuits. The striatum is a critical gateway between the cortex and other deep brain structures, coordinating decision making, motivation, reward perception, reinforcement, and motor planning (36). The predominant affection of the executive and limbic subsections of this neural node in combination with changes of strongly myelinated WM in the anterior part of the corpus callosum and mesial temporal structures as the parahippocampal and fusiform gyrus found in our study corroborates previous findings of modest, but significant cognitive decrement in T1D (37). Furthermore, the absence of cortical atrophy previously reported in several studies (19–22), including in our previous study sharing a part of the

Table 2—Anatomical localization of clusters in the VBM analysis and T1w/T2w ratio analysis, log-*P* scale

Cluster number	Structure	%	Volume (voxels)	−log-*P* value (FWE)	MNI coordinates of local maxima		
					x	*y*	*z*
VBM: control subjects without diabetes > patients with T1D							
1	L putamen	91	356	1.59	73	96	46
2	R putamen	99	124	1.48	44	82	54
T1w/T2w ratio: patients with T1D > control subjects without diabetes							
1	R thalamus	30	1,310	2.03	48	58	43
	L thalamus	20					
	R putamen (*executive segment*)	16					
2	L cerebellum, lobule VII, VIII, crus II		259	1.89	23	31	11
3	R cerebellum, lobule VII, VIII, crus II		104	1.84	58	37	8
4	L putamen (*executive segment*)	85	100	1.97	57	68	37
5	L, R cerebellum, lobules I-IV		82	1.85	39	43	26

Clusters are significant at $P < 0.05$ FWE voxelwise corrected for the VBM analysis and at $P < 0.05$ FWE and Bonferroni corrected for the T1w/T2w ratio analysis, with the cluster threshold of 50 contiguous voxels. Striatal subsegmentation provided in italics with percent coverage of the respective cluster in striatum. Only substructures covering at least 10.0% of the respective cluster are listed in the table. L, left; R, right.

subject cohort, is perplexing. However, the fully congruent results of the analysis of cortical thickness in surface reconstructions, VBM, and ROI volumes bring reasonable confidence in our conclusion and data-driven inference on the absence of macrostructural cortical changes at a group level in this cohort.

In addition to the adverse effects of episodic hypoglycemia and hyperglycemia, further pathophysiological mechanisms need to be considered as possible instigators of these micro- and macrostructural changes. Even though the character and locality of changes in striatum and thalamus as detected in the T1w/T2w ratio analysis is highly suggestive of vascular nature since these deep areas are supplied through an end-arterial system, our primary hypothesis of microvascular-mediated lower cerebral blood perfusion in patients with T1D was not supported by the absence of any significant regional differences in CBF values comparing patients with T1D and control subjects without diabetes. Because impaired cerebrovascular responsiveness in patients with T1D with disease duration >10 years (38) is to be expected and the mean disease duration in our T1D cohort of 21 years was well above this threshold (only 9 of 63 included patients had shorter disease duration), one may search for the possible cause of the absence of CBF changes in good blood glucose control (mean HbA_{1c} of 7.4%, range 5.6–13.6%, with only 3 subjects presenting a value >9% the day of the study), hyperinsulinemia state during image acquisition, or minimal extent of blood perfusion changes below the sensitivity of arterial spin labeling MRI (39). Furthermore, although rare, the diabetic striatal disease (40) implicates certain vulnerability of this structure to blood glucose excess. The higher ratio of GABA-ergic neurons, which are particularly sensitive to metabolic stress (41), also has been hypothesized as one of the major contributors (42). Importantly, previously implicated selective changes in other subtypes of GABA-ergic interneurons in hippocampus (43) may well be linked with the alterations detected in our study. Finally, the autoimmune character of the disease must be acknowledged, where the lower tissue fidelity of autoreactive T cells in diabetes plays a significant role as a possible mechanism of CNS damage (44).

Nonetheless, several points need to be considered with regard to our results. First, as emphasized above, T1w/T2w ratio is a compound parameter that reflects multiple possible alterations, including cortical myelin changes, edema, and iron content. Although it is not possible to provide more specific deductions about the nature of the T1w/T2w changes observed in this study, it provides a reasonable rationale for further research designed to distinguish the character of the observed changes. Second, the absence of detailed neurocognitive testing prevents us from inferring more precise conclusions on the character and clinical implications of the observed macrostructural and microstructural changes. Also, no cognition screening was performed, although no subjects included in the study referred subjective cognitive impairment. Further studies that focus on the correlation of various MRI measures with neuropsychological parameters should be particularly rewarding. Third, although the longitudinal character of both neuroimaging data and information on blood glucose control and disease development is desirable, such studies are highly impractical, if even feasible. The cross-sectional character of the study also complicates the interpretation of the negative outcome of the secondary analysis correlating disease duration with imaging data. Multiple study-related factors may have played a role, such as number of

Table 3—FreeSurfer volumetry outcomes in the ROIs

ROI	Control subjects without diabetes, mean ± SD (range)	Patients with T1D, mean ± SD (range)	Difference (T1D − control), %	*P* value uncorrected	*P* value Holm corrected
Caudate	0.0051 ± 0.0006 (0.00404–0.00715)	0.0049 ± 0.0006 (0.00358–0.00639)	−3.5	0.069	0.550
Putamen	**0.0071 ± 0.0009 (0.00478–0.00901)**	**0.0067 ± 0.0008 (0.00491–0.00831)**	**−6.3**	**0.003**	**0.025**
Pallidum	0.0018 ± 0.0003 (0.00094–0.00259)	0.0018 ± 0.0002 (0.00134–0.00227)	−2.9	0.281	1
Hippocampus	0.0033 ± 0.0002 (0.00284–0.00398)	0.0033 ± 0.0003 (0.00215–0.00398)	1.2	0.495	1
Cerebellum	0.070 ± 0.007 (0.0575–0.0892)	0.069 ± 0.006 (0.0547–0.0843)	−0.7	0.730	1
Frontal cortex	0.13 ± 0.02 (0.095–0.164)	0.13 ± 0.02 (0.081–0.170)	−0.5	0.613	1
Parietal cortex	0.08 ± 0.01 (0.059–0.103)	0.08 ± 0.01 (0.051–0.110)	−1.3	0.375	1
Occipital cortex	0.035 ± 0.005 (0.0252–0.0460)	0.034 ± 0.005 (0.0226–0.0486)	−1.8	0.259	1
Temporal cortex	0.08 ± 0.01 (0.058–0.104)	0.08 ± 0.01 (0.049–0.113)	0.0	0.716	1
Thalamus	**0.0105 ± 0.0009 (0.00790–0.01304)**	**0.0098 ± 0.0008 (0.00780–0.01161)**	**−6.3**	**0.000**	**0.000**
Whole cortex	0.34 ± 0.02 (0.308–0.397)	0.34 ± 0.02 (0.282–0.442)	−1.1	0.27	NA

Volumes were determined by FreeSurfer segmentation and were adjusted by the estimated intracranial volume. *P* values refer to group comparisons as described in the RESEARCH DESIGN AND METHODS. Significant differences are highlighted in bold. NA, not applicable.

subjects, inclusion criteria, and range of disease duration in individual patients, to name a few. Again, long-term longitudinal data would be required to answer this question adequately. On the other hand, it is highly probable that the absence of significant correlations between HbA_{1c} levels and imaging data is related to the narrow range of HbA_{1c} level as an inclusion criterion for patients with T1D. The negative results in the CBF analysis may reflect a true absence of major flow differences and/or may be "artificial" because of the hyperinsulinemic clamp in the study protocol. Finally, the absence of intergroup cortical volume differences might be considered surprising since a part of the present study cohort was shared with a previous study reporting cortical volume decrease (21). As confirmed by much more similar results in our auxiliary analysis that included only subjects shared by both studies, the divergent outcomes might be explained by differences both in the groups and in the processing software used.

Table 4—CBF outcomes in the ROIs

ROI	Control subjects without diabetes, mean ± SD (range)	Patients with T1D, mean ± SD (range)	Difference (T1D − control), %	*P* value uncorrected	*P* value Holm corrected
Caudate	44 ± 10 (17–70)	44 ± 11 (25–70)	1.3	0.834	1
Putamen	51 ± 9 (37–78)	52 ± 10 (29–72)	0.4	0.924	1
Pallidum	40 ± 8 (24–66)	41 ± 10 (21–69)	2.1	0.757	1
Hippocampus	57 ± 11 (31–81)	55 ± 10 (38–77)	−3.5	0.22	1
Frontal cortex	69 ± 11 (47–98)	68 ± 14 (41–97)	−0.3	0.841	1
Parietal cortex	72 ± 14 (40–105)	68 ± 15 (40–102)	−4.9	0.114	0.796
Occipital cortex	73 ± 15 (40–114)	69 ± 14 (39–98)	−5.5	0.095	0.763
Temporal cortex	63 ± 11 (40–90)	62 ± 11 (37–90)	−1.3	0.578	1
Thalamus	55 ± 13 (32–100)	51 ± 10 (31–79)	−7.1	0.035	0.313
Whole cortex	68 ± 12 (43–96)	67 ± 13 (40–96)	−2.3	0.376	NA

P values refer to group comparisons as described in the RESEARCH DESIGN AND METHODS. CBF units are mL/100 g/min. NA, not applicable.

In conclusion, our findings highlight the marked nonvascular disruption of several essential neural nodes engaged in both cognitive and motor processing, providing a biologically plausible model of the hypothesized diabetic encephalopathy in T1D. The pooled outcomes of the current study and previous research in T1D implicate the combination of relatively subtle, but definite differences in brain structure as an organic basis and mild changes in cognitive performance. Although the pathogenesis of these macrostructural and microstructural alterations is obscure as of now, its detailed delineation will be an important goal.

Acknowledgments. The authors are grateful to the volunteers who participated in the study and thereby made this research possible. The authors are also grateful to the MRI support available at the Center for Magnetic Resonance Research (namely, Erik Solheid and Wendy Elvendahl) and the support of the nurses (Michelle Snyder and Kathryn France). In addition, the authors thank Dr. Alena Svatkova for helpful suggestions on data processing and Nathan Rubin for help with data entry. The authors acknowledge the Minnesota Supercomputing Institute at the University of Minnesota for providing resources that contributed to the research results reported within this article (https://www.msi.umn.edu).

Funding. Research reported in this article was supported by the National Institutes of Health (award numbers P41-EB-015894, P30-NS-076408, R01-DK-099137, and R56-DK-099137) and by the National Center for Advancing Translational Sciences of the National Institutes of Health (award numbers KL2-TR-000113 and UL1-TR-000114). Research reported in this publication was also supported by the European Union H2020 Marie Skłodowska-Curie Actions RISE project #691110 (MICROBRADAM).

The content is solely the responsibility of the authors and does not necessarily represent the official views of the funding agencies.

Duality of Interest. No potential conflicts of interest relevant to this article were reported.

Author Contributions. P.F. performed the T1w/T2w ratio and volumetry analyses and wrote the manuscript. A.C. performed the CBF analysis and reviewed and edited the manuscript. A.M. and A.F.K. recruited the study subjects and reviewed the manuscript. P.B. and H.G. participated in the study and analysis design and reviewed the manuscript. X.L. designed the MRI acquisition protocol and reviewed the manuscript. E.O. and L.E.E. designed the statistical methods and reviewed the manuscript. E.R.S. designed the study, secured funding, and reviewed and edited the manuscript. S.M. designed the study, secured funding, analyzed and interpreted the data, and reviewed and edited the manuscript. S.M. is the guarantor of this work and, as such, had full access to all the data in the study and takes responsibility for the integrity of the data and the accuracy of the data analysis.

References

1. Brands AM, Biessels GJ, de Haan EH, Kappelle LJ, Kessels RP. The effects of type 1 diabetes on cognitive performance: a meta-analysis. Diabetes Care 2005; 28:726–735

2. Rovet J, Ehrlich R, Hoppe M. Behaviour problems in children with diabetes as a function of sex and age of onset of disease. J Child Psychol Psychiatry 1987;28: 477–491

3. Ryan C, Longstreet C, Morrow L. The effects of diabetes mellitus on the school attendance and school achievement of adolescents. Child Care Health Dev 1985;11:229–240

4. Dejgaard A, Gade A, Larsson H, Balle V, Parving A, Parving H-H. Evidence for diabetic encephalopathy. Diabet Med 1991;8:162–167

5. Boeve BF, Bell DG, Noseworthy JH. Bilateral temporal lobe MRI changes in uncomplicated hypoglycemic coma. Can J Neurol Sci 1995;22:56–58

6. Wautier J-L, Schmidt AM. Protein glycation: a firm link to endothelial cell dysfunction. Circ Res 2004;95:233–238

7. Ceriello A. Oxidative stress and glycemic regulation. Metabolism 2000; 49(Suppl. 1):27–29

8. Navedo MF, Takeda Y, Nieves-Cintrón M, Molkentin JD, Santana LF. Elevated Ca2+ sparklet activity during acute hyperglycemia and diabetes in cerebral arterial smooth muscle cells. Am J Physiol Cell Physiol 2010;298:C211–C220

9. Beauquis J, Homo-Delarche F, Revsin Y, De Nicola AF, Saravia F. Brain alterations in autoimmune and pharmacological models of diabetes mellitus: focus on hypothalamic-pituitary-adrenocortical axis disturbances. Neuroimmunomodulation 2008;15:61–67

10. Castillo-Gómez E, Coviello S, Perez-Rando M, et al. Streptozotocin diabetic mice display depressive-like behavior and alterations in the structure, neurotransmission and plasticity of medial prefrontal cortex interneurons. Brain Res Bull 2015;116:45–56

11. Lovett-Barron M, Losonczy A. Behavioral consequences of GABAergic neuronal diversity. Curr Opin Neurobiol 2014;26:27–33

12. Taplin CE, Barker JM. Autoantibodies in type 1 diabetes. Autoimmunity 2008; 41:11–18

13. Barker JM, Yu J, Yu L, et al. Autoantibody "subspecificity" in type 1 diabetes: risk for organ-specific autoimmunity clusters in distinct groups. Diabetes Care 2005;28:850–855

14. Vianello M, Tavolato B, Armani M, Giometto B. Cerebellar ataxia associated with anti-glutamic acid decarboxylase autoantibodies. Cerebellum 2003;2:77–79

15. Perros P, Deary IJ, Sellar RJ, Best JJ, Frier BM. Brain abnormalities demonstrated by magnetic resonance imaging in adult IDDM patients with and without a history of recurrent severe hypoglycemia. Diabetes Care 1997;20:1013–1018

16. Ferguson SC, Blane A, Wardlaw J, et al. Influence of an early-onset age of type 1 diabetes on cerebral structure and cognitive function. Diabetes Care 2005; 28:1431–1437

17. Nunley KA, Ryan CM, Orchard TJ, et al. White matter hyperintensities in middle-aged adults with childhood-onset type 1 diabetes. Neurology 2015;84: 2062–2069

18. Yousem DM, Tasman WS, Grossman RI. Proliferative retinopathy: absence of white matter lesions at MR imaging. Radiology 1991;179:229–230

19. Musen G, Lyoo IK, Sparks CR, et al. Effects of type 1 diabetes on gray matter density as measured by voxel-based morphometry. Diabetes 2006;55:326–333

20. Hughes TM, Ryan CM, Aizenstein HJ, et al. Frontal gray matter atrophy in middle aged adults with type 1 diabetes is independent of cardiovascular risk factors and diabetes complications. J Diabetes Complications 2013;27:558–564

21. Bednarik P, Moheet AA, Grohn H, et al. Type 1 diabetes and impaired awareness of hypoglycemia are associated with reduced brain gray matter volumes. Front Neurosci 2017;11:529

22. Wessels AM, Simsek S, Remijnse PL, et al. Voxel-based morphometry demonstrates reduced grey matter density on brain MRI in patients with diabetic retinopathy. Diabetologia 2006;49:2474–2480

23. Moulton CD, Costafreda SG, Horton P, Ismail K, Fu CHY. Meta-analyses of structural regional cerebral effects in type 1 and type 2 diabetes. Brain Imaging Behav 2015;9:651–662

24. Hershey T, Perantie DC, Wu J, Weaver PM, Black KJ, White NH. Hippocampal volumes in youth with type 1 diabetes. Diabetes 2010;59:236–241

25. Ho MS, Weller NJ, Ives FJ, et al. Prevalence of structural central nervous system abnormalities in early-onset type 1 diabetes mellitus. J Pediatr 2008;153:385–390

26. van Elderen SGC, Brandts A, van der Grond J, et al. Cerebral perfusion and aortic stiffness are independent predictors of white matter brain atrophy in type 1 diabetic patients assessed with magnetic resonance imaging. Diabetes Care 2011;34:459–463

27. Glasser MF, Van Essen DC. Mapping human cortical areas in vivo based on myelin content as revealed by T1- and T2-weighted MRI. J Neurosci 2011;31: 11597–11616

28. Beer A, Biberacher V, Schmidt P, et al. Tissue damage within normal appearing white matter in early multiple sclerosis: assessment by the ratio of T1- and T2-weighted MR image intensity. J Neurol 2016;263:1495–1502

29. Mangia S, Tesfaye N, De Martino F, et al. Hypoglycemia-induced increases in thalamic cerebral blood flow are blunted in subjects with type 1 diabetes and hypoglycemia unawareness. J Cereb Blood Flow Metab 2012; 32:2084–2090
30. Glasser MF, Sotiropoulos SN, Wilson JA, et al.; WU-Minn HCP Consortium. The minimal preprocessing pipelines for the Human Connectome Project. Neuroimage 2013;80:105–124
31. Postelnicu G, Zollei L, Fischl B. Combined volumetric and surface registration. IEEE Trans Med Imaging 2009;28:508–522
32. Canna A, Ponticorvo S, Russo AG, et al. A group-level comparison of volumetric and combined volumetric-surface normalization for whole brain analyses of myelin and iron maps. Magn Reson Imaging 2018;54:225–240
33. Ashburner J. A fast diffeomorphic image registration algorithm. Neuroimage 2007;38:95–113
34. Shen S, Sterr A. Is DARTEL-based voxel-based morphometry affected by width of smoothing kernel and group size? A study using simulated atrophy. J Magn Reson Imaging 2013;37:1468–1475
35. Winkler AM, Ridgway GR, Webster MA, Smith SM, Nichols TE. Permutation inference for the general linear model. Neuroimage 2014;92:381–397
36. Yager LM, Garcia AF, Wunsch AM, Ferguson SM. The ins and outs of the striatum: role in drug addiction. Neuroscience 2015;301:529–541
37. Ferguson SC, Blane A, Perros P, et al. Cognitive ability and brain structure in type 1 diabetes: relation to microangiopathy and preceding severe hypoglycemia. Diabetes 2003;52:149–156
38. Fülesdi B, Limburg M, Bereczki D, et al. Impairment of cerebrovascular reactivity in long-term type 1 diabetes. Diabetes 1997;46:1840–1845
39. Petcharunpaisan S, Ramalho J, Castillo M. Arterial spin labeling in neuroimaging. World J Radiol 2010;2:384–398
40. Abe Y, Yamamoto T, Soeda T, et al. Diabetic striatal disease: clinical presentation, neuroimaging, and pathology. Intern Med 2009;48:1135–1141
41. Kann O. The interneuron energy hypothesis: implications for brain disease. Neurobiol Dis 2016;90:75–85
42. Larsson M, Lietzau G, Nathanson D, et al. Diabetes negatively affects cortical and striatal GABAergic neurons: an effect that is partially counteracted by exendin-4. Biosci Rep 2016;36:e00421
43. Yi SS. Time-dependent changes of calbindin D-28K and parvalbumin immunoreactivity in the hippocampus of rats with streptozotocin-induced type 1 diabetes. J Vet Sci 2013;14:373–380
44. Winer S, Astsaturov I, Cheung R, et al. Type I diabetes and multiple sclerosis patients target islet plus central nervous system autoantigens; nonimmunized nonobese diabetic mice can develop autoimmune encephalitis. J Immunol 2001; 166:2831–2841